Journal of Environmental Management 298 (2021) 113538

Contents lists available at ScienceDirect

Journal of Environmental Management

journal homepage: www.elsevier.com/locate/jenvman

BDD electrochemical oxidation of neonicotinoid pesticides in natural surface waters. Operational, kinetic and energetic aspects

Joaquin R. Domínguez *, Teresa González, Sergio Correia

Department of Chemical Engineering and Physical Chemistry. Area of Chemical Engineering. Faculty of Sciences, University of Extremadura, Avda. de Elvas, s/n, Badajoz, 06006, Spain

A R T I C L E I N F O

Keywords:
Electrochemical oxidation
BDD electrodes
Neonicotinoid pesticides
Depuration
Natural surface waters
Wastewater treatment plant effluent

A B S T R A C T

Neonicotinoids pesticides were introduced to the market in the 1990s to control various pests. Its accumulation in the environment supposes a severe problem that can affect human health. This study investigates the electrochemical degradation of four common neonicotinoid pesticides; thiamethoxam (TMX), imidacloprid (ICP), acetamiprid (ACP) and thiacloprid (TCP), in different natural surface waters by a boron-doped diamond anode (BDD). The most influencing variable was the current density (j), and to a lesser extent, the supporting electrolyte concentration (C_e). In optimal conditions (j = 34.14 mA cm^{-2} and C_e = 10.00 mM, using Na_2SO_4 as electrolyte) pesticide removals for TMX, ICP, ACP and TCP were 97.2, 96.9, 87.8 and 98.2 %, respectively. The obtained results with different support electrolytes (Na_2SO_4, NaCl, $NaNO_3$ and HK_2PO_4) suggest that sulphate electrolyte was the optimum for TMX, ICP and ACP. However, for TCP, a total removal was achieved in less than 10 min using NaCl. It was also verified that the initial pH of the solution did not significantly influence the process in the range 3–9. All these results were rationalized in this paper. Finally, to evaluate the matrix influence, some experiments were carried out in different natural surface water matrices (river, reservoir and two different WWTP effluents). The factors influencing the process were the conductivity of the solution and the organic matter content. It was noticeable that the specific energy consumption (SEC) reduced by approximately 15 % for river water and WWTP effluent. High mineralization rates were obtained for all water matrices, with TOC removals ranging between 60 and 80 %.

1. Introduction

Electro-oxidation (EO) (also known as electrochemical oxidation) by specific electrodes have been widely studied to degrade different pollutants such as pharmaceuticals (García-espinoza et al., 2018), dyes (Costa et al., 2009; Tang et al., 2020), personal care and hygiene products (Pueyo et al., 2020), pesticides (Carboneras Contreras et al., 2020), surfactants (Louhichi et al., 2008), steroids and hormones (Nájera-Aguilar et al., 2016), among others. In this way, the organic compounds present in the solution reaches total mineralization (CO_2) or degrades into simpler forms and less polluting compounds. Considering that advanced electrochemical oxidation processes (EAOPs) are low-cost and high-efficiency technologies, they have attracted increasing attention. Not only for the degradation of a wide variety of pollutants but also in reducing the total organic content (TOC) of different pollution sources. They have also been considered environmentally friendly (Chen et al., 2020; Ouarda et al., 2019; Rajasekhar et al., 2020; Turan et al., 2020).

Additionally, boron-doped diamond electrode (BDD) has emerged as a new anodic material due to its exciting properties (Panizza and Cerisola, 2005). This new material competes with conventional anode electrodes (Pt, IrO_2, RuO_2), which present different limitations, such as O_2 evolution potential below 1.8 V/SHE and lower efficiency (Cai et al., 2020; Comninellis, 1994; Feng et al., 2014). Boron-doped diamond thin-film anode brings technologically essential characteristics such as an inert surface with low adsorption properties, remarkable corrosion stability, and broad potential windows in the aqueous medium. These properties confer to the BDD-anode a much greater O_2 overvoltage than a conventional anode such as Pt, allowing the production of a higher amount of reactive hydroxyl radicals. This material has been considered the best "non-active" anode material that interacts so weakly with the ·OH radicals, allowing the direct oxidation of organics. This material also competes with graphite electrode (which presents a rapid loss of activity), PbO_2 (present leaching risks), and SnO_2 (which present a short helpful life) (Costa et al., 2009; Ganiyu et al., 2016).

* Corresponding author.
E-mail address: jrdoming@unex.es (J.R. Domínguez).

https://doi.org/10.1016/j.jenvman.2021.113538
Received 29 April 2021; Received in revised form 13 July 2021; Accepted 10 August 2021
Available online 14 August 2021

Neonicotinoid pesticides (NCTs) includes a group of insecticides introduced to the international market in the 1990s. They have been used to control a wide variety of pests in agriculture, horticulture, forestry, among others (Simon-Delso et al., 2015). This group includes 13 compounds (imidacloprid, acetamiprid, thiacloprid, nitenpyram, clothianidin, thiamethoxam, dinotefuran, flupyradifurone, imidacloprid, sulfoxaflor, paichongding, cycloxaprid and guadipyr) (Simon-Delso et al., 2015). These NCT compounds have demonstrated important environmental adverse effects due to their high solubility in water and stability in the soil (Bonmatin et al., 2015). A significant risk was associated with the accumulation of these pesticides in the non-target organisms. Recent studies have shown that aquatic ecosystems and soils can act as NCTs transport routes due to their common use to control various crops' pests (Aseperi et al., 2020; Bonmatin et al., 2021; Montiel-León et al., 2019; Sjerps et al., 2019). Among these most relevant adverse effects related to the use of these insecticides, the harmful effects on various organisms has been demonstrated (Cycoń et al., 2013; English et al., 2021; Humann-Guilleminot et al., 2019; Lopez-Antia et al., 2015; Tasman et al., 2021). Additionally, Zhang et al. (2019) detected NCTs in Chinese urine samples collected throughout the country. The mean concentrations in urine, expressed in ng·mL^{-1}, was 0.24, 0.21, 0.15 and 0.14 ng mL^{-1} for clothianidin, imidacloprid, thiamethoxam and dinotefuran, respectively. Due to these harmful effects, four of these NCT compounds (clothianidin, imidacloprid, thiacloprid and thiamethoxam) were included on 2015 in the list of priority substances to be removed from continental waters in the European Union (European Comisssion, 2020).

Consequently, it is necessary to contribute to developing more effective treatment technologies to remove these pollutants. This work presents exciting results on the degradation of four neonicotinoid compounds; thiamethoxam (TMX), imidacloprid (ICP), acetamiprid (ACP) and thiacloprid (TCP) using boron-doped diamond anode (BDD). The influence of the current density (j) and the concentration of support electrolyte (C_e) were studied using a statistical design of experiments. Other environmental conditions such as pH, electrolyte nature, electrolyte concentration, among others, were also checked. Finally, some experiments were carried out in different natural surface water matrices (such as river water, swamp water and two WWTP effluents) to study the influence of the aqueous matrix.

2. Materials and methods

2.1. Materials

NCTs compounds, thiamethoxam, imidacloprid, acetamiprid, and thiacloprid were supplied by Sigma-Aldrich with a purity >98 % for all cases. NaCl, Na_2SO_4, $NaNO_3$ and K_2HPO_4 salts were purchased with a purity >99 % from PanreacQuimica. The mobile phase used for HPLC analysis was a mixture of acetonitrile (ACN) (PanreacQuímica), and ultrapure water (UPW) obtained from a Millipore Milli-Q system (resistivity: 18.2 MΩ cm^{-1} to 25 °C and TOC content ≤ 5 ppb) acidified with formic acid (Merck). For buffered pH solutions, the pH was adjusted with H_3PO_4 and K_2HPO_4 (PanreacQuimica). All chemicals were used as received without additional purification.

2.2. Real surface-water matrices

NCTs degradation was investigated in ultrapure water (UPW) and four natural surface water matrices: water collected from the Guadiana River (RW-1), water from the Villar del Rey public reservoir (RW-2), water from Almendralejo WWTP (RW-3), and effluent from Badajoz WWTP (RW-4). These water matrices were filtered through PET filters of 0.45 μm, and stored at the dark in a refrigerator at 4 °C for later use. The characterization of these real surface-water matrices is shown in Table 1.

2.3. Experimental installation

The experimental installation used for electrochemical oxidation processes is shown in Figure S1 (Supplemental Material). The experiments were carried out in a single compartment electrochemical reactor consisting of two circular electrodes of 100 mm in diameter (geometric area of 78 cm^2) with a gap of 9 mm. A boron-doped diamond anode (BDD) and a stainless-steel cathode (AISI 304) were used. The BDD electrode was supplied by CSEM (Switzerland). Electrolysis was performed using a power supply (Tektronix PWS2326), which allows operation at a maximum intensity of 6 A with a potential range 0–32 V. The solution containing NCTs mixture (TMX, ICP, ACP, and TCP with a concentration for each one equal to 1 μM) was introduced into the reaction system. The used volume for each experience was always 350 mL. The solution is circulated throughout the installation, passing the electrochemical reactor and cooling column until returning to the tank using two peristaltic pumps (SelectaPercom N-M) operating at a flow rate of 250 cm^3 min^{-1}. Also, a thermoregulatory water bath (OVAN Bath Cryostat model BC10E) with heating and refrigerating capacity was used to maintain the reaction temperature at 20 ± 0.1 °C. The sampling of 1.0 mL at different time intervals (0, 2, 5, 10, 15, 20, 30, 45 and 60 min) was performed for posterior HPLC analysis. Moreover, to remove possible BDD-surface impurities, and before electrolysis, the electrodes were polarized with 10 mM Na_2SO_4 solution at a current density (j) of 20 mA cm^{-2} for 15 min.

2.4. Sample analysis

NCTs degradation by electrochemical oxidation was followed by high-resolution liquid chromatography (HPLC) in reverse phase using an Agilent 1260 Infinity II chromatograph equipped with a PDA detector. Quantifications were performed at 254 nm for TMX, ACP and TCP, and 270 nm for ICP injecting 100 μL aliquots into the LC system. The stationary phase was a C18 column of 5 μm, 150 mm and 4.6 mm internal

Table 1
Main physicochemical properties of real surface water matrices.

	RW-1 (Guadiana River)	RW-2 (Villar del Rey Reservoir)	RW-3 (Almendralejo WWTP effluent)	RW-4 (Badajoz WWTP effluent)
pH	7.95	8.11	8.72	7.57
Conductivity (μS·cm^{-1})	640	151	2332	540
Turbidity (NTU)	0.58	0.44	0.98	0.61
TOC (mg·L^{-1})	7.04	8.69	20.04	9.66
COD (mg O_2·L^{-1})	22.4	26.8	60.7	29.7
Total phosphorus (mg P·L^{-1})	0.06	0.05	0.99	1.27
Total nitrogen (mg N·L^{-1})	2.3	1.6	11.6	12.1
Nitrate (mg NO_3^-·L^{-1})	8.5	1.3	30.5	23.7
Nitrite (μg NO_2^-·L^{-1})	51	634	57	621
Ammonium (mg NH_4^+·L^{-1})	0.23	0.78	1.17	3.87
A_{254nm} (cm^{-1})	0.135	0.140	0.559	0.183
Total solids (mg·L^{-1})	360	250	1690	410
Fixed solids (mg·L^{-1})	285	175	1390	325
Volatile solids (mg·L^{-1})	75	75	300	85

diameter at 25 °C. The mobile phase used was a mixture of UPW (acidified with 0.2 % v/v formic acid) and ACN in gradient mode operating at a flow rate 1.0 mL min^{-1}. The initial volumetric ratio of the mobile phase was 85:15 for 1.25 min. A linear gradient was then applied for 3.75 min to the UPW-ACN mixture until it reached a ratio of 70:30, which was maintained for 2 min. Finally, the equipment returns to the initial isocratic conditions with a stabilization time of 3 min. The total time for each analysis was 10 min. Well defined peaks were obtained for TMX, ICP, ACP and TCP at 5.07, 6.47, 7.51 and 8.75 min, respectively.

Total organic carbon (TOC) analysis was determined using an Analytikjena Multi N/C® 3100 analyzer. Chemical oxygen demand (COD) was analyzed using Hach Lange vials in the range 5–60 mg $O_2 \cdot L^{-1}$ (Cl^- concentration in the real water samples was always below 2 g L^{-1}, as recommended by the manufacturer (see Table 1)). A Lange LT-200 thermostat was used for the digestion of samples. The total content of phosphorus, nitrogen, nitrate, nitrite and ammonia were determined by Hanna kits using a Hanna HI83399 photometer.

Total solids (TS), volatile solids (VS), and fixed solids (FS) were determined using a gravimetric method (Sartorius model CP224S). Parameters such as pH, conductivity and temperature were measured with a multiparametric meter (Hanna, model HI 255).

3. Results and discussion

3.1. Influence of operating variables

A statistical design of experiments was planned to establish the influence of operating variables on the process. Experimental runs were carried out modifying current density (j) and electrolyte concentration (C_e) (independent variables), following a Composite Central Design (CCD) model. This design has 5 levels per factor (-α, −1, 0, +1, +α), where -α and +α are the minimum and maximum axial points, −1 and +1 the minimum and maximum factorial points, and 0 the centre point. This configuration allows investigating linear, quadratic and interaction effects between independent variables. For this design, α value is 1.41, resulting in a total number of experiments equal to 16, with 8 replicates of the centre point. This system meets the orthogonality and rotability criteria and ensures that the studied effects vary equally in all directions (See Table S1: Supplementary Material).

The degradation efficiency (E_i), expressed as the NCT removal percentage (Eq. (1)), the apparent pseudo-first-order kinetic rate constant (k_i) (Eq. (2)), and the specific energy consumption (SEC, kWh·μM^{-1}) (Eq. (3)) were chosen as target variables. The response surface methodology (RSM) was used to analyze the interaction between electrochemical process parameters (j and C_e) on each target response. This methodology allows mathematical modelling of the relationship between input variables and output variables, analyzing them and adjusting them to a polynomial equation (Eq. (4)). The validity of the selected and applied model was supported by the variance analysis (test ANOVA). Table S1 (Supplementary Material) shows the operating conditions of each experiment, and Table S2 the obtained results.

$$E_i = \left(\frac{C_o - C}{C_o}\right) 100 \tag{1}$$

$$ln\left(\frac{C_o}{C}\right) = k_i \cdot t \tag{2}$$

$$\mathrm{SEC} = \frac{E_{cell} \cdot I \cdot t}{3600 \cdot V \cdot (C_o - C)} \tag{3}$$

Where C_o is the initial concentration of each neonicotinoid compound (μM), C is the concentration at different reaction times (μM), t is the reaction time (min), E_{cell} is the applied cell potential (V), I is the current intensity (A), and V is the volume of the treated solution (dm^3).

$$Y = b_0 + \sum_{i=1}^{n} b_i X_i + \sum_{i=1}^{n} b_{ii} X_i^2 + \sum_{i=1}^{n-1} \sum_{j=i+1}^{n} b_{ij} X_i X_j \tag{4}$$

Being Y the target variable (E_i, k_i or SEC), X_i, X_i^2, and X_iX_j are the effects of independent variables, square effects, and interaction effects, respectively, b_i, b_{ii}, and b_{ij} are the polynomial interaction coefficients of the linear, quadratic, and second-order terms, respectively, and b_0 is the polynomial independent term.

3.1.1. Removal efficiency and kinetics as target variables

Table S2 (Supplementary Material) lists the removal percentages and apparent pseudo-first-order kinetic rate constant for each NCT compound. Moreover,Table S3and Table S4 (Supplementary Material) show the ANOVA analysis for target variables (E_i and k_i). All factors with a p-value below 0.05 have a significant influence on the target variable. As is shown, the current density (j), its squared value (j^2), as well as the electrolyte concentration (C_e) significantly influence the NCTs removal with a probability of 95 %. Also, the interaction between current density and the electrolyte concentration (j-C_e) significantly influences TCP degradation (p-Values < 0.0196).

On the other hand, the coefficients' absolute values (Eq. (4)) inform us about each variable specific weight on the target variable. The higher the value, the more significant is this variable; the positive or negative sign indicates the favourable or unfavourable influence on the target variable. Equations (Eqs. (5)–(8)) show the coefficients obtained by adjusting the experimental results to a polynomial equation for TMX, ICP, ACP and TCP removal percentages (%), respectively. The response surface and the contour plot curves for each NCT compound are shown in Fig. 1.

$$E_{TMX}\ (\%) = 90.56 + 7.863 \cdot j + 2.407 \cdot C_e - 2.519 \cdot j^2 \tag{5}$$

$$E_{ICP}\ (\%) = 88.36 + 8.836 \cdot j + 3.151 \cdot C_e - 2.252 \cdot j^2 \tag{6}$$

$$E_{ACP}\ (\%) = 70.08 + 16.32 \cdot j + 4.662 \cdot C_e - 3.004 \cdot j^2 \tag{7}$$

$$E_{TCP}\ (\%) = 90.76 + 11.88 \cdot j + 3.558 \cdot C_e - 1.839 \cdot jC_e - 5.162 \cdot j^2 \tag{8}$$

Similarly, Eqs. (9)–(12) were obtained considering as target variable the pseudo-first-order kinetic rate constant. For this case, the current density and the support electrolyte concentration significantly influences this target variable. The interaction between current density and electrolyte concentration influences all neonicotinoids except ACP, whereas the value of the squared density and squared electrolyte concentration exerts a positive influence on the elimination rate of ICP and TCP. From multiple regression analysis, the response surface and the contour plot curves for each NCT compound are shown in Figure S2 (Supplementary Material).

$$k_{TMX}\ (min^{\overline{1}}) = 0.0409 + 0.0130 \cdot j + 0.0050 \cdot C_e + 0.0019 \cdot jC_e \tag{9}$$

$$k_{ICP}\ (min^{\overline{1}}) = 0.0359 + 0.0128 \cdot j + 0.0045 \cdot C_e + 0.0019 \cdot jC_e + 0.0013 \cdot j^2 + 0.0012 \cdot C_e^2 \tag{10}$$

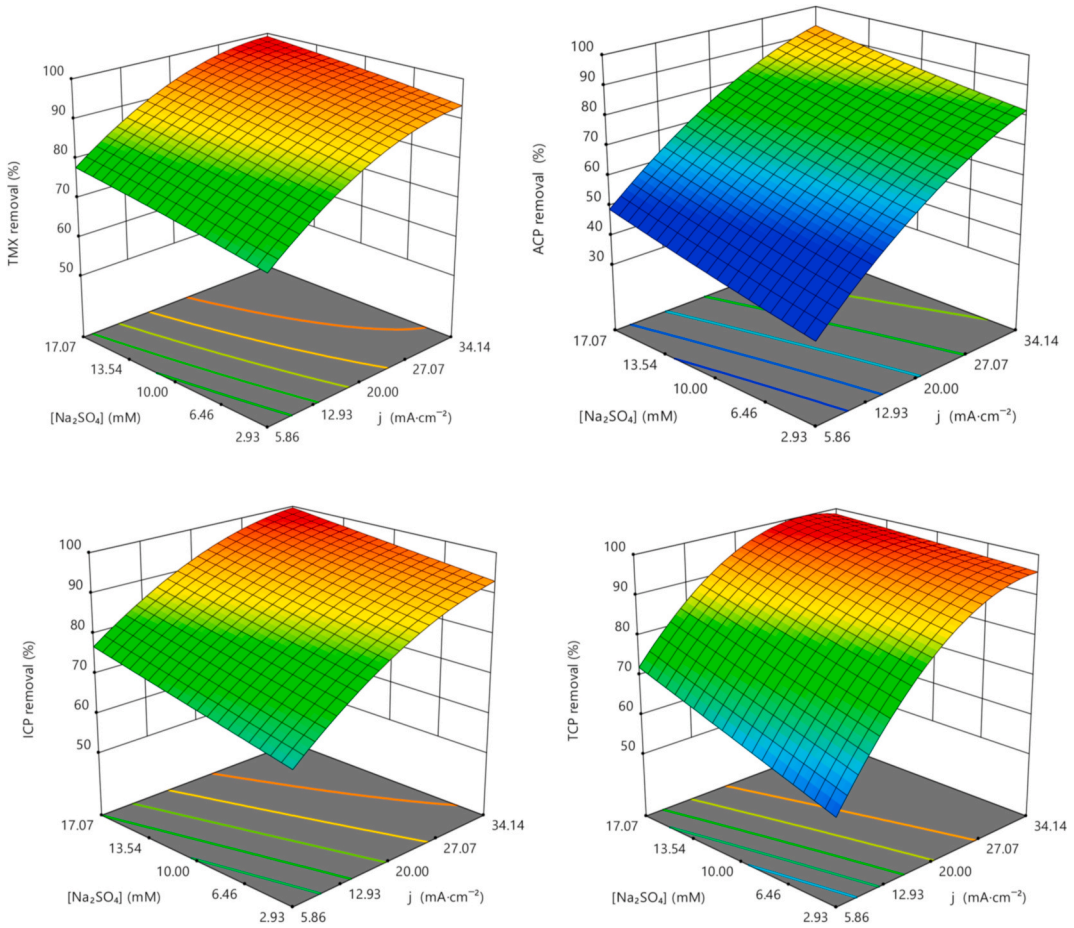

Fig. 1. Estimated response surface and level curves for removing TMX, ICP, ACP and TCP by electro-oxidation. Operating variables (j) and (C_e).

$$k_{ACP}\ (min^{\overline{1}}) = 0.0202 + 0.0090 \cdot j + 0.0028 \cdot C_e + 0.0009 \cdot j^2 \quad (11)$$

$$k_{TCP}\ (min^{\overline{1}}) = 0.0405 + 0.0192 \cdot j + 0.0070 \cdot C_e + 0.0028 \cdot jC_e + 0.0015 \cdot j^2 + 0.0010 \cdot C_e^2 \quad (12)$$

As shown in Fig. 1, NCTs removal was favoured by higher j values. Current density is a parameter directly related to the number of generated oxidizing species. An increase in current density leads to an increase of electrogenerated reactive oxygen species (ROS), mainly hydroxyl radicals BDD ($^{\bullet}$OH) (see Eq. (13)), other less reactive radicals BDD ($HO_2^{\bullet}$) (Eq. (17)), and also indirect oxidants as H_2O_2 (Eq. (16)). Consequently, an increase in applied current density would lead to a better electron transfer rate by increasing NCT degradation (direct oxidation pathway) (Tang et al., 2020). Moreover, as the current density (j) increases, the diffusion flow of organic matter to the anode surface increases, decreasing the diffusion layer's thickness and improving the process (Samet et al., 2010).

$$BDD + H_2O \rightarrow BDD(^{\bullet}OH) + H^+ + e^- \quad (13)$$

$$BDD(^{\bullet}OH) + H_2O \rightarrow BDD + O_2 + 3H^+ + 3e^- \quad (14)$$

$$2BDD(^{\bullet}OH) \rightarrow 2BDD + O_2 + 2H^+ + 2e^- \quad (15)$$

$$2BDD(^{\bullet}OH) \rightarrow 2BDD + H_2O_2 \quad (16)$$

$$BDD(^{\bullet}OH) + H_2O_2 \rightarrow BDD(HO_2^{\bullet}) + H_2O \quad (17)$$

Concerning the obtained statistical results, an increase of current from 5.86 to 34.14 mA cm^{-2} (EO-1 and EO-12 experiments) improved TMX degradation from 72.9 % to 97.2 % (see Table S2, Supplementary Material). This trend was also observed for ICP, ACP and TCP, reaching removals close to 100 % for the highest current density. However, this increase in NCTs removal efficiency is not linearly proportional. There are two contrary effects; as the j value increases, the hydroxyl radicals production also increases (Eq. (13)); however, the undesirable reactions (parasitic reactions) on the electrodes' surface also increases. These parasitic reactions consume some of the BDD ($^{\bullet}$OH) radicals generated, decreasing the radical concentration available to oxidize the pesticides. Among them, the oxidation of BDD ($^{\bullet}$OH) radicals to O_2 (Eqs. (14) and (15)) significantly reduces the process's energy efficiency. A relatively high current density will also produce a greater amount of gas on the electrodes' surface (H_2 and O_2, in the cathode and anode, respectively) by decreasing the contaminant oxidation rate. On the other hand, BDD ($^{\bullet}$OH) dimerization (E° = +2.80 V) to H_2O_2 (E° = +1.78 V) generates less reactive species (Eq. (16)), and even the destruction of BDD ($^{\bullet}$OH) radicals to produce less reactive BDD ($HO_2^{\bullet}$) radicals (E° = +1.70 V)

(Eq. (17)).

These obtained results are consistent with those obtained by Ganiyu et al. (2016) for the degradation of a 0.1 mM amoxicillin solution using an increasing current from 30 to 120 mA. The mineralization efficiency increased with current from 27 to 94 %, but they observed a significant reduction in oxidation efficiency at high current values (between 60 and 120 mA). TOC reduction increased by 14 % compared to 30 % obtained when the current increased from 30 to 60 mA. Similar results were obtained by Zazou et al. (2017) in the degradation of the herbicide 2,4, 5-trichloro-phenoxy-acetic acid using a current between 300 and 1000 mA. Complete degradation was achieved after 40 min of reaction using 1000 mA compared to the required time (55 and 70 min) when the current intensity was 500 and 300 mA, respectively.

Regarding electrolyte concentration (Na_2SO_4), the results confirm a positive effect (minor than current density) on process efficiency. An increase of C_e implies a higher conductivity and an improvement in the medium electron transfer capacity (high mobility of ions in solution) (Nidheesh and Gandhimathi, 2012). On the other hand, direct oxidation of the electrolyte species (i.e. NaCl, Na_2SO_4, Na_2CO_3, Na_3PO_4) may occur on the anode surface to generate radicals, which can be combined to produce more stable oxidants (Sirés et al., 2014). For this case, SO_4^{2-} anions present in the medium can be oxidized directly to radical sulphate anions ($SO_4^{-\bullet}$) on the anode surface (Eq. (18)). Electrogenerated $SO_4^{-\bullet}$ radicals can be combined to produce more stable oxidants such as persulfate ($S_2O_8^{2-}$) (Eq. (19)) (Sirés et al., 2014). An increase in the concentration of Na_2SO_4 implies a more significant amount of electrogenerated $SO_4^{-\bullet}$ radicals and, therefore, a greater efficiency.

$$SO_4^{2-} \rightarrow \left(SO_4^{-}\right)^{\bullet} + e^{-} \quad (18)$$

$$\left(SO_4^{-}\right)^{\bullet} + \left(SO_4^{-}\right)^{\bullet} \rightarrow S_2O_8^{2-} \quad (19)$$

$$2HSO_4^{-} \rightarrow S_2O_8^{2-} + 2H^{+} + 2e^{-} \quad (20)$$

The results obtained in the experiences with the same current intensity j (20 mA cm^{-2}) and different electrolyte doses (2.93, 10 and 17.07 mM, EO-4, EO-2 and EO-9 experiments) show this growing trend in removal efficiency - i.e., TCP degradation increased from 84.7 % to 95.4 % by increasing Na_2SO_4 concentration- (see Table S2, Supplementary Material). The same behaviour was observed for all neonicotinoids. Additionally, this electrolyte influence was more remarkable for small current densities. Fig. 2 shows the influence of the electrolyte concentration (5–15 mM) on TCP removal at different current densities (j = 10–30 mA cm^{-2}).

Several authors have studied the effect of electrolyte concentration

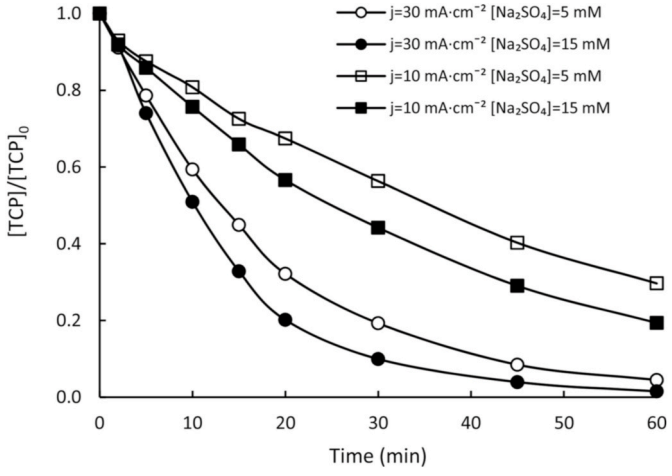

Fig. 2. Evolution of the normalized TCP concentration over time. Influence of electrolyte concentration (5–15 mM Na_2SO_4) for different j values (10–30 mA cm^{-2}).

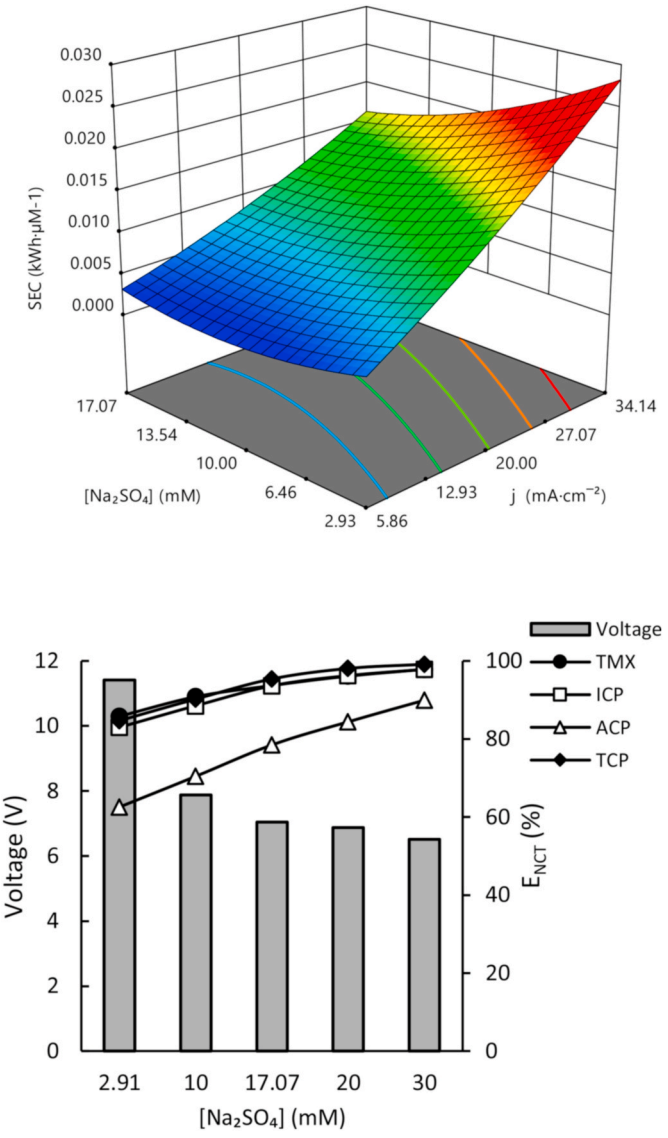

Fig. 3. Estimated response surface and contours plots for SEC parameter (top). Influence of electrolite concentration (Na_2SO_4) on the applied voltage (bar diagram) and NCTs removal (bottom). Experimental conditions: j = 20 mA cm^{-2}, C_i = 1 µM, V = 350 mL and T = 20 °C.

(Na_2SO_4) on the degradation of different organic compounds by electrooxidation. As an example, Tang et al. (2020) investigated the influence of Na_2SO_4 (in the range 0.025–0.1 M) on the degradation of yellow X-6G dye. An increase in the supporting electrolyte concentration improved the colour bleaching rate due to a higher hydroxyl radical generation and a greater contribution of indirect oxidation by $S_2O_8^{2-}$ (Eq. (19) and (20)). However, the removal percentages reached at 1.25 h were practically similar (90.2, 94.7, 96.2 and 99.6 % for electrolyte concentrations 25, 50, 75 and 100 mM, respectively). Also, Cai et al. (2020) concluded that the concentration of Na_2SO_4 in the range 5–100 mM for the degradation of 2.4-dichloro-phenoxy-acetic acid was insignificant (the elimination percentages obtained after 120 min of treatment were in the range 91–98 %). Similarly, Barışçı et al. (2018) found that an increase in the support electrolyte concentration (Na_2SO_4) from 100 to 200 ppm increased the rate of degradation of carboplatin; however, an increase to 300 ppm was unfavourable.

3.1.2. SEC parameter as target variable

SEC parameter, specific energy consumption, kWh·µM^{-1} (see Eq.

(3)) was determined for each experiment to evaluate their economic viability. Fig. 3 (top) shows the response surface and level curves for the SEC parameter as a function of the operating variables j and C_e. The SEC parameter values were also shown in Table S2 (Supplementary Material).

Under higher current density, higher SEC values were obtained. An increase in the current density j implies an increase in the applied E_{cell}, therefore, in the SEC parameter. For experiments with j values of 5.86, 20 and 34.14 mA cm^{-2} (EO-1, EO-2 and EO-12), the applied potential increased from 5.01 V to 10.07 V (increasing SEC parameter by a factor of 12). However, the NCTs removal efficiency increased only by a factor of 1.6 (see Fig. 3). These results can be explained by considering secondary reactions (Eqs. (14)–(17)), significantly reducing the process's energy efficiency. Also, the presence of more gas bubbles (hydrogen and oxygen) on the electrodes' surface would decrease the disponibility of active sites (for one hand) and hinder the matter transfer of contaminants to electrodes (for the other hand). These two factors favour unwanted reactions, decreasing energy efficiency (especially at long reaction times).

Regarding the influence of the electrolyte on the SEC value, this parameter decreases at higher electrolyte concentrations. An increase in the electrolyte concentration means a higher conductivity of the solution, and therefore a decrease in the cell voltage (see Eq. (3)) (Tang et al., 2020). The results obtained in experiments carried out with the same j value (20 mA cm^{-2}) and different doses of Na_2SO_4 (2.93, 10, 17.07, 20 and 30 mM) show different E_{cell} voltages (Fig. 3 (bottom)). However, this decrease in voltage with increasing C_e is not linear, being very important up to 10–17 mM. Upper values do not affect the cell voltages significantly. Similar results were obtained by Turan et al. (2020) for thiocyanate electro-oxidation. They established a minimum value of electrolyte concentration of 0.5 g L^{-1} (3.52 mM) for a feasible electrochemical treatment (from an economic point of view).

Table S5 (Supplementary Material) shows the variance analysis for the SEC parameter. All the factors that present a p-value below 0.05 exert a significant influence. In this case, all the variables (j and C_e) and their squared values (j^2 and C_e^2), as well as the interaction between the current density and electrolyte concentration ($j \cdot C_e$), significantly influence this parameter.

The adjustment of the experimental values to a polynomial equation appears in the following expression (Eq. (21)):

$$SEC\ \left(kWh\ \mu mol^{-1}\right) = 0.010334 + 0.006450 \cdot j - 0.002410 \cdot C_e - 0.001268 \cdot jC_e + 0.000496 \cdot j^2 - 0.000933 \cdot C_e^{\,2} \quad (21)$$

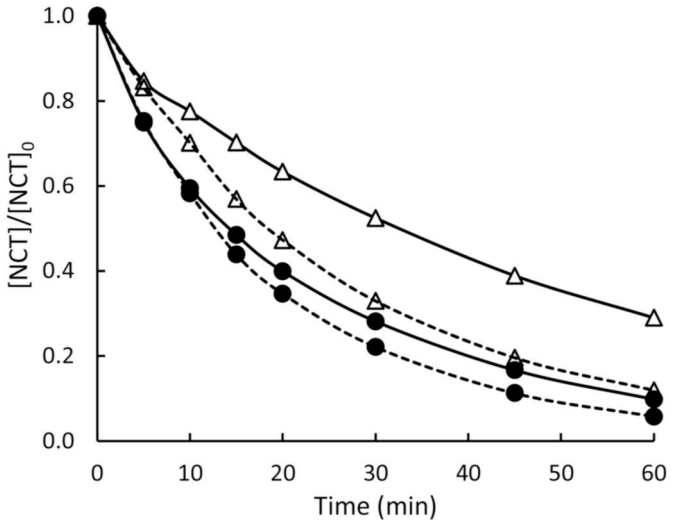

Fig. 4. Evolution of the normalized concentration of TMX (circle) and ACP (triangle). Influence of the presence of other NCTs pesticides: in mixture (continuous line) or individually (dashed line). Experimental conditions. J = 20 mA cm^{-2}, C_i = 1 μM, V = 350 mL and T = 20 °C.

3.2. Influence of the presence of other pesticides

This section analyzes the results obtained for the NCT degradation in individuals and the mixture. The experimental conditions for this study were: j = 20 mA cm^{-2}, $[Na_2SO_4]$ = 10 mM, C_i = 1 μM, V = 350 mL and T = 20 °C (that corresponds the experimental conditions of the center point (0, 0) of the design of experiments). The solution pH resulted from mixing the contaminants in UPW was approximately pH = 6. Fig. 4 shows the evolution of the normalized concentration of neonicotinoids TMX and ACP with time. For all cases, C_i = 1 μM and ΣC_i = 4 μM (for the mixture). Table S6 shows the elimination percentages reached at 60 min of reaction time and the pseudo-first-order kinetic constants. Concerning the reactivity of neonicotinoids, the obtained rank order was TCP = TMX = ICP > ACP.

As is shown in Fig. 4, the degradation rate for individual solutions was greater than in the mixture. The absence of other NCTs in the solution implies a greater amount of available ROS, mainly BDD ($^{\bullet}OH$) radicals, to degrade the target compound, compared to experiences in solutions containing the mixture. For this case, the removal percentages at 60 min increased from 90.2 to 94.2 %, 88.0–94.0 %, 71.0–88.1 % and 90.8–95.4 %, for TMX, ICP, ACP and TCP, respectively. For the ACP case, the pseudo-first-order kinetic rate constant increased from 0.021 to 0.036 min^{-1}. This significant improvement for this compound (the most recalcitrant) may be explained as follows. The removal achieved for TMX, ICP and TCP compounds was very similar in individual as in mixture solutions, showing a very high reactivity with ROS. However, for ACP (significantly less reactive), the presence of other more reactive neonicotinoids affected more remarkably.

Regarding the specific energy consumption, as was expected, the SEC parameter decreases in the mixture. Although the removal percentage in individual experiments was higher, total NCTs removal increases in the mixture for the same current dose.

3.3. Influence of electrolyte nature and concentration

The electrolyte plays a crucial role in solutions without sufficient conductivity since it provides a higher conductivity and improves the electron transfer in the medium (Nidheesh and Gandhimathi, 2012). In addition, the electrolyte nature could also be an influencing factor in the process efficiency. Different inorganic anions such as SO_4^{2-}, Cl^-, PO_4^{3-} can react by generating other more stable oxidants (Lan et al., 2017; Pueyo et al., 2020). For these reasons, some experiments were carried out modifying the electrolyte nature (Na_2SO_4, NaCl, $NaNO_3$ and HK_2PO_4) and its concentration (10, 20 and 30 mM). Table S7 lists the NCTs removal percentages reached at 60 min, as well as the values of the apparent pseudo-first-order kinetic rate constant (Eq. (2)). For all cases, the kinetic data suggest a pseudo-first-order model with correlation coefficients close to one ($R^2 > 0.99$).

Fig. 5 shows the evolution of normalized TCP concentration for experiments carried out with different electrolytes and doses. Similarly,

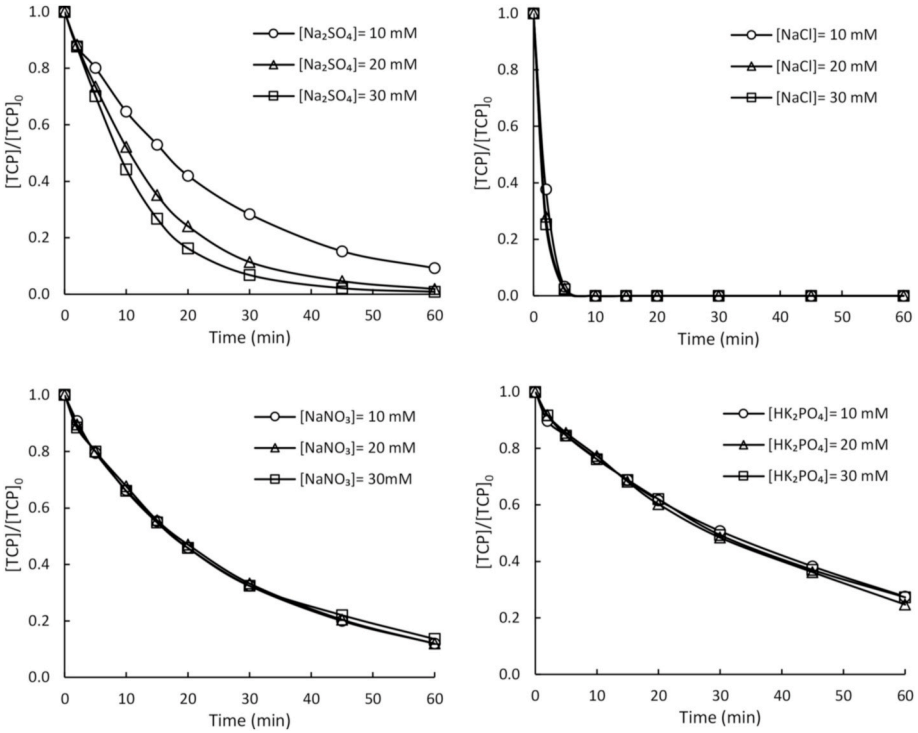

Fig. 5. Normalized TCP concentration versus time. Influence of electrolyte nature and concentration. Experimental conditions: j = 20 mA cm^{-2}, C_i = 1 μM, V = 350 mL and T = 20 °C.

Figures S3, S4 and S5 (Supplementary Material) collect the results obtained for TMX, ICP and ACP.

The influence of the Na_2SO_4 concentration has already been studied in section 3.1.1. As was shown, an increase in electrolyte concentration leads to higher degradation rates. The most significant influence was observed for the most recalcitrant pollutant, ACP.

The use of NaCl as an electrolyte implies the electro-generation of chlorine gas (indirect oxidant) (see Eq. (22)). The chlorine gas generated dissolves in the aqueous phase to generate OCl^-/HOCl (Eq. (23) and (24)), both powerful oxidants. The presence of these two species will depend on the pH. HOCl is predominant for pHs between 3 and 8 and OCl^- for pHs>8 (Sirés et al., 2014). As is shown in Fig. 5, total TCP removal was speedy (approx. 5 min) compared with other electrolytes (>60 min). These results can be explained considering the indirect oxidation of chlorine species (Cl_2, HClO and ClO^-).

$$2Cl^- \rightarrow Cl_2 + 2e^- \quad (22)$$

$$Cl_2 + H_2O \rightleftarrows HOCl + H^+ + Cl^- \quad (23)$$

$$HOCl \rightleftarrows OCl^- + H^+ \quad (24)$$

In contrast, for ICP, the results were the opposite to this trend. Decreasing pseudo-first-order k values of 0.0391, 0.0357 and 0.0289 min^{-1} were obtained for increasing NaCl concentrations 10, 20 and 30 mM, respectively (see Table S7; Supplementary Material). No significant influence was observed for ACP and TMX.

In this connection, Yin et al. (2018) studied the degradation of ICP and TCP by chlorine, UV, and UV/chlorine. These authors observed that the addition of Cl^- in the UV/chlorine system significantly promoted TCP degradation and slightly inhibited ICP degradation. They concluded that TCP was degraded by reactive radicals (i.e., $^{\bullet}OH$, $Cl^{\bullet}$ and $Cl_2^{\bullet-}$) and free chlorine. Therefore, the electro-generation of chlorine gas at the anode during the electro-oxidation treatment would be the main cause of this improvement. Authors thought that this TCP rapid degradation could be attributed to forming a similar chlorinated molecule. In the present investigation, a new intense peak with a retention time equal to

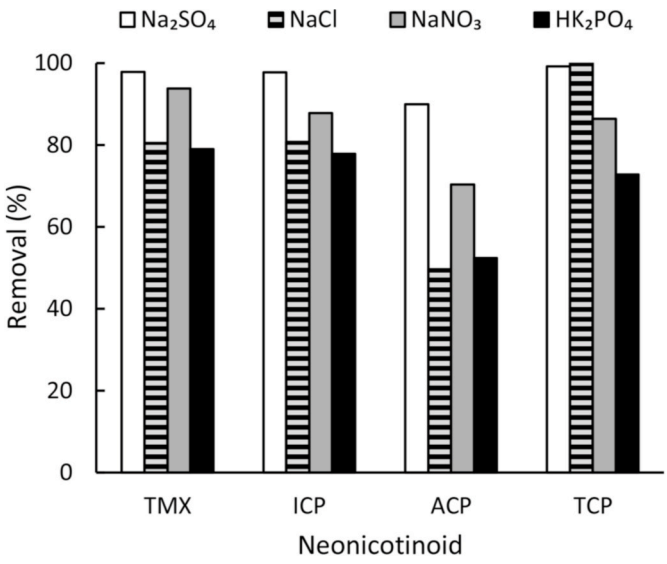

Fig. 6. NCTs removal after 60 min of reaction. Influence of the electrolyte (C_e = 30 mM). Experimental conditions: j = 20 mA cm^{-2}, C_i = 1 μM, V = 350 mL and T = 20 °C.

5.70 min was observed in the HPLC chromatogram. This peak remained visible up to 15 min of treatment and was attributed to a chlorinated oxidation intermediate since it generally requires long electrolysis times to be degraded.

Regarding the influence of $NaNO_3$ concentration, no influence was observed on any of the NCTs. Similar pseudo-first-order apparent kinetic constants were obtained for different electrolyte concentrations. In conclusion, the use of $NaNO_3$ as a supporting electrolyte increases the conductivity of the solution but does not generate secondary oxidants (Jardak et al., 2016; Lakshmipathiraj et al., 2012). In other words, in

UPW + NO_3^- solution, NCTs degradation is carried out only by ROS (mainly BDD ($^{\bullet}OH$)).

The presence of PO_4^{3-} in the medium could influence NCTs degradation in different ways. In this work, NCTs removal percentages and apparent kinetic rate constants were lower in the presence of PO_4^{3-}. This fact may be explained considering the scavenger effect of the phosphate anion. This undesirable effect can justify the observed decrease in NCTs removal and k values. On the other hand, as was reported by Cañizares et al. (2005), peroxodiphosphate anion $P_2O_8^{4-}$ (a powerful oxidant) (Eq. (25)) can be generated by electro-oxidation. However, pH turns out to be an essential variable. These same authors studied the concentration of $P_2O_8^{4-}$ generated electrochemically at different pH values, establishing an optimal pH = 12–13. Also, Costa et al. (2009) investigated the degradation of acid black dye 210 by electrochemical oxidation using a BDD anode in the presence of phosphate. For this case, the best results were obtained at pH = 11.7. In this investigation, initial pH values were 9.55, 9.68 and 9.71 for electrolyte doses of 10, 20 and 30 mM, respectively. These values were consistently below those reported in the literature for the formation of peroxodiphosphate anion.

$$2PO_4^{3-} \rightarrow P_2O_8^{4-} + 2e^- \quad (25)$$

Finally, to compare the influence of the support electrolyte nature on the process efficiency, Fig. 6 shows the NCTs removal percentage after 60 min of reaction for different electrolytes. As can be seen, for the TMX, ICP and ACP, the highest elimination percentages are reached using Na_2SO_4, followed by $NaNO_3$ and NaCl. These best results with Na_2SO_4 can be justified by considering other secondary sulphate oxidants (Eqs. (18)–(20)) (indirect oxidants). Analyzing the results obtained for Na_2SO_4 and $NaNO_3$ and attributing only oxidation by ROS in the $NaNO_3$ media, it can be concluded that generated sulphate species also play an important role in the NCTs degradation. These results agree with those obtained by other authors in the degradation of other organics. Lakshmipathiraj et al. (2012) investigated the effect of the electrolyte on the anodic oxidation of trichloroethene. Their results showed a complete elimination using Na_2SO_4 compared to 92 % achieved in the presence of $NaNO_3$. Similarly, Jardak et al. (2016) obtained lower efficiencies in the electrochemical degradation of ethylene glycol. Organic removals achieved after 120 min of reaction were 50.1 and 89.4 %, using $NaNO_3$ and Na_2SO_4, respectively.

Regarding TCP compound, the pseudo-first-order k values were approximately 10 times greater in NaCl solutions (0.5113, 0.6576 and 0.7491 min^{-1} for NaCl concentrations of 10, 20 and 30 mM) compared with the Na_2SO_4 media (0.0410, 0.0694 and 0.072 min^{-1}). Electrogenerated chloride reactive species during electrochemical treatment can attack pollutants in competition with $^{\bullet}OH$ radicals. These species are more selective and can react with electron-rich moieties more rapidly than $^{\bullet}OH$ (García-espinoza et al., 2018) as occurs for TCP.

For all neonicotinoids, the lowest efficiency was obtained using HK_2PO_4 as electrolyte. Its radical scavenger effect on ROS hindered its use as a supporting electrolyte.

3.4. Influence of pH

The studied pH range was 3–9, which implies that all neonicotinoid compounds are in molecular form. To maintain constant the pH, a buffer H_3PO_4/K_2HPO_4 30 mM was used. All experiments were performed with a j value of 20 mA cm^{-2} and a Na_2SO_4 concentration of 10 mM. Table 2 shows the apparent pseudo-first-order k values obtained in each experiment for all neonicotinoids.

Table 2
Apparent pseudo-first-order k values obtained in each experiment for all neonicotinoids.

System	k_{TMX} (min^{-1})	k_{ICP} (min^{-1})	k_{ACP} (min^{-1})	k_{TCP} (min^{-1})
without buffer	0.0404	0.0357	0.0212	0.0410
pH 3	0.0312	0.0322	0.0155	0.0280
pH 5	0.0326	0.0338	0.0167	0.0308
pH 7	0.0329	0.0341	0.0185	0.0339
pH 9	0.0327	0.0328	0.0171	0.0355

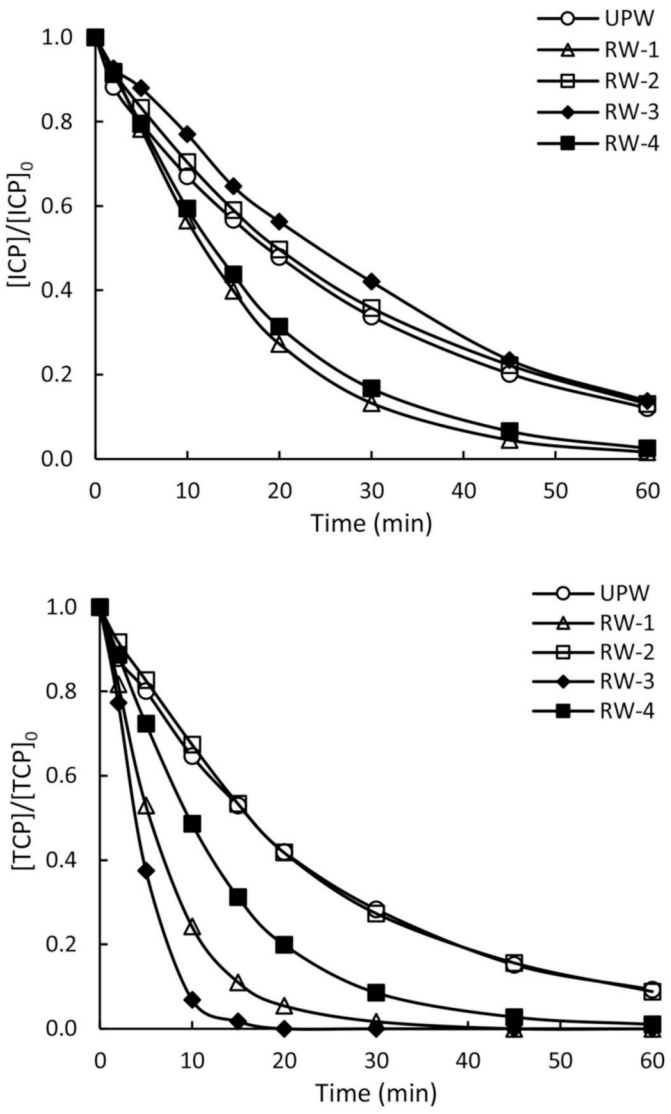

Fig. 7. Evolution of the normalized concentration of ICP (top) and TCP (bottom). Influence of the aqueous matrix. Experimental conditions: j = 20 mA cm^{-2}, C_i = 1 μM, [Na_2SO_4] = 10 mM, V = 350 mL and T = 20 °C.

In general, the initial pH of the solution did not significantly influence the process (in the range 3–9). The apparent pseudo-first-order k values increase smoothly when increasing pH between 5 and 7. Above pH 7, the k values decreased slightly except for TCP. However, the highest k values were obtained for no buffered solutions. With the natural pH of the solution (approximately 6), the degradation rate was maximum. As was explained in the previous section, PO_4^{3-} anions present in the medium act as radical scavengers. Similar results were obtained by Frontistis et al. (2017) for the degradation of ethylparaben for the same pH range (3–9).

3.5. Influence of the aqueous matrix

In the previous sections, NCTs degradation was studied in UPW, the simplest matrix with a negligible organic content (TOC ≤ 5 ppb), using Na_2SO_4 as support electrolyte, at a pH of approximately 6 (natural pH of

the mixture). However, it is necessary to study the behaviour of this systems in natural aqueous matrices. The complexity of the aqueous matrix is a parameter that can affect the efficiency of the process. On the one hand, the inorganic ions present in surface waters can generate different reactive species (secondary oxidants) that can indirectly participate in the degradation of neonicotinoids. In this connection, different reactive species can be generated from sulphates ($SO_4^{-\bullet}$ and $S_2O_8^{2-}$), chloride (Cl_2, HClO, ClO^-, $Cl^\bullet$ and $Cl_2^{\bullet-}$), phosphates ($P_2O_8^{4-}$), and even carbonates ($CO_3^{\bullet-}$ and $C_2O_6^{2-}$). This section studies NCTs degradation in four real surface water matrices: river (RW-1), reservoir (RW-2), Almendralejo WWTP effluent (RW-3), and Badajoz WWTP effluent (RW-4). The main physicochemical properties of these surface waters are shown in Table 1. Fig. 7 shows the evolution of normalized NCT concentration with time for ICP (top) and TCP (bottom) in different aqueous matrices. Similarly, the evolution of the normalized concentrations of TMX and ACP are shown in Figure S6 (Supplementary Material).

Table S8 (Supplementary Material) shows the apparent pseudo-first-order kinetic rate constant and the SEC parameter for each NCT compound in the different aqueous matrices. As is shown, the nature of the aqueous matrix significantly influences the degradation rate. Two clearly and differentiated behaviours were distinguished. On the one hand, TMX, ICP, and ACP presented a similar trend, with the following reactive sequence RW-1 > RW-4 > UPW > RW-2 > RW-3, being the most recalcitrant ACP for all cases. ICP and TMX presented a similar behaviour for all water matrices, except for the more organic loaded (RW-3). On the other hand, the sequence of reactivity for TCP was different RW-3 > RW-1 > RW-4 > RW-2 ~ UPW.

Regarding the first group (TMX, ICP and ACP), NCTs removal efficiency was more remarkable in effluents RW-1 and RW-4, with lower organic content (TOC = 7,0–9,6 mg L^{-1}) and a moderate conductivity (540–640 μS cm^{-1}). This effect may be explained by considering the inorganic species (sulphate, chloride, nitrate, phosphate and carbonate) that improve the electron transfer in the medium, for one hand, and the possible electro generation of secondary reactive species (secondary oxidants) by another.

Based on these criteria, it should be expected that the results obtained for RW-3 would be the best. However, natural organic matter content (NOM) negatively affects the process by occupying active sites on the surface of the electrodes and competing with NCTs compounds for reactive species. The high TOC content of RW-3 effluent (21.0 mg L^{-1}) and the low conductivity of RW-2 (107.2 μS cm^{-1}) penalize the efficiency in these aqueous matrices. In this connection, Pueyo et al. (2020) studied the influence of humic acids content (HA) on the degradation of ethylparaben. They observed the same negative effect of the HA content on the process.

On the contrary, regarding TCP, higher degradation rates were found in the more complex matrices. This effect can be due to the chloride content in these effluents that favours the formation of secondary oxidants such Cl_2, HClO, ClO^-, $Cl^\bullet$ and $Cl_2^{\bullet-}$. This improvement was already commented on in section 3.3 when using NaCl as a supporting electrolyte.

Regarding the energy consumed for different aqueous matrices, the value of the SEC parameter was determined for all cases at 60 min (see Eq. (3)) (see Table S8: Supplementary Material). The obtained results indicate that energy costs decreased when natural surface waters were used, except for reservoir effluent (RW-2), due to its low conductivity (RW-2 and UPW conductivity after adding the same amount of Na_2SO_4 were very similar). In this way, the SEC parameter decreases for two reasons: firstly, the presence of inorganic species increases conductivity, decreasing the value of the applied cell potential (E_{cell}), and secondly, due to the contribution of electrogenerated reactive species. For example, the specific energy consumption, expressed in kWh·μmol^{-1}, is reduced by approximately 15 % for the RW-1 and RW-4 compared to UPW.

Finally, the mineralization capacity (measured as TOC reduction) was analyzed for each aqueous matrix. Fig. 8 shows the evolution of TOC over time for the different surface water matrices. The results indicated that EO treatment supposes a very interesting process, not only to degrade NCTs compounds but also to purify and improve the quality of the real surface effluent, achieving TOC reductions of 58.56, 64.80, 73.95 and 79.03 % for RW-1, RW-2, RW-3 and RW-4, respectively.

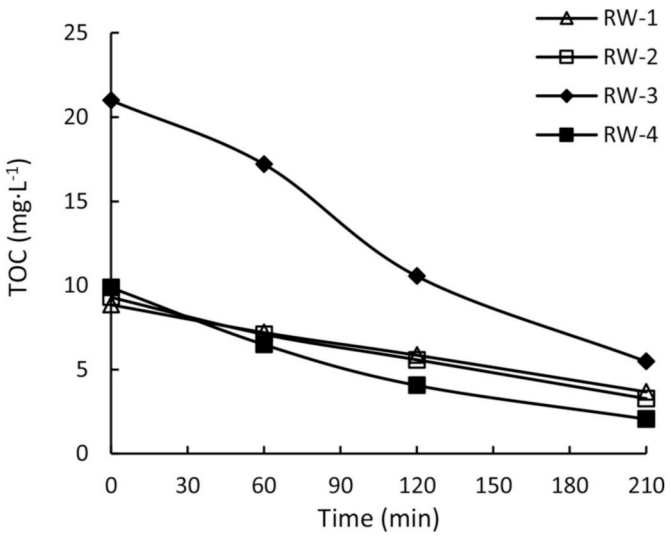

Fig. 8. Evolution of TOC content with time. Influence of the aqueous matrix. Experimental conditions: j = 20 mA cm^{-2}, C_i = 1 μM, [Na_2SO_4] = 10 mM, V = 350 mL and T = 20 °C.

4. Conclusions

The results obtained indicate that electro-oxidation treatment would be a suitable process to remove neonicotinoids pesticides in natural surface waters. Among the independent variables studied (current density and concentration of support electrolyte), the most significant effect on degradation kinetics was the applied current density. The concentration of support electrolyte also influences, although to a lesser extent. In the central operating conditions of the design, the elimination percentages achieved for TMX, ICP, ACP and TCP were 90.2, 88.0, 71.0 and 90.8 %, respectively.

The process energy consumption was evaluated with the SEC parameter. An increase in current density (j) and a decrease in electrolyte concentration (C_e) significantly increased the energy costs. For the central point of the design, an SEC value of 0.0103 kWh·μM^{-1} was obtained.

Except for TCP, the highest degradation rates were obtained using Na_2SO_4 as electrolyte. For TCP, a fast removal was obtained in NaCl solution in less than 10 min. The electrogenerated reactive chlorine species (Cl_2, HClO, ClO^-, $Cl^\bullet$ and $Cl_2^{\bullet-}$) can explain this. The pH of the solution to be treated had little effect on the efficiency of the electrochemical treatment. Also, the phosphate-buffer scavenger effect may hinder any concrete conclusion about pH effect.

For real water matrices, the nature of the water matrix had a significant influence on the efficiency of the process. Inorganic ions increased the conductivity of water and contributed positively; however, the natural organic matter content (measured as TOC) reduces the process efficiency. It was possible to reduce the SEC parameter by approximately 15 % for RW-1 and RW-4 water matrices compared to UPW. Also, it was achieved significant mineralization rates (measured as TOC reduction) for the different effluents in the range 60–80 %.

Credit author statement

Joaquín R. Dominguez: Supervision, Writing – original draft preparation, Conceptualization, Methodology, Writing-Reviewing and Editing; Teresa Gonzalez: Conceptualization, Methodology, Writing – original draft preparation, Writing-Reviewing and Editing, Sergio Correia: Writing – original draft preparation, Investigation, Validation.

Declaration of competing interest

The authors declare that they have no known competing financial interests or personal relationships that could have appeared to influence the work reported in this paper.

Acknowledgements

The authors gratefully acknowledge financial support of this research work through the Comisión Interministerial de Ciencia y Tecnología (CICYT)-CTM 2016-75873-R project-as well as through Junta de Extremadura under GR18043 and IB16016 projects and Fondo Europeo de Desarrollo Regional and Plan Propio de Iniciación a la Investigación, Desarrollo Tecnológico e Innovación de la Universidad de Extremadura.

Appendix A. Supplementary data

Supplementary data to this article can be found online at https://doi.org/10.1016/j.jenvman.2021.113538.

References

Aseperi, A.K., Busquets, R., Hooda, P.S., Cheung, P.C.W., Barker, J., 2020. Behaviour of neonicotinoids in contrasting soils. J. Environ. Manag. 276, 111329. https://doi.org/10.1016/j.jenvman.2020.111329.

Barışçı, S., Turkay, O., Ulusoy, E., Soydemir, G., Seker, M.G., Dimoglo, A., 2018. Electrochemical treatment of anti-cancer drug carboplatin on mixed-metal oxides and boron doped diamond electrodes: density functional theory modelling and toxicity evaluation. J. Hazard Mater. 344, 316–321. https://doi.org/10.1016/j.jhazmat.2017.10.029.

Bonmatin, J.M., Giorio, C., Girolami, V., Goulson, D., Kreutzweiser, D.P., Krupke, C., Liess, M., Long, E., Marzaro, M., Mitchell, E.A., Noome, D.A., Simon-Delso, N., Tapparo, A., 2015. Environmental fate and exposure; neonicotinoids and fipronil. Environ. Sci. Pollut. Res. 22, 35–67. https://doi.org/10.1007/s11356-014-3332-7.

Bonmatin, J.M., Mitchell, E.A.D., Glauser, G., Lumawig-Heitzman, E., Claveria, F., Bijleveld van Lexmond, M., Taira, K., Sánchez-Bayo, F., 2021. Residues of neonicotinoids in soil, water and people's hair: a case study from three agricultural regions of the Philippines. Sci. Total Environ. 757, 143822. https://doi.org/10.1016/j.scitotenv.2020.143822.

Cai, J., Zhou, M., Pan, Y., Lu, X., 2020. Degradation of 2,4-dichlorophenoxyacetic acid by anodic oxidation and electro-Fenton using BDD anode: influencing factors and mechanism. Separ. Purif. Technol. 230, 115867. https://doi.org/10.1016/j.seppur.2019.115867.

Cañizares, P., Larrondo, F., Lobato, J., Rodrigo, M.A., Sáez, C., 2005. Electrochemical synthesis of peroxodiphosphate using boron-doped diamond anodes. J. Electrochem. Soc. 152, D191. https://doi.org/10.1149/1.2039936.

Carboneras Contreras, M.B., Villaseñor Camacho, J., Fernández-Morales, F.J., Cañizares, P.C., Rodrigo Rodrigo, M.A., 2020. Biodegradability improvement and toxicity reduction of soil washing effluents polluted with atrazine by means of electrochemical pre-treatment: influence of the anode material. J. Environ. Manag. 255 https://doi.org/10.1016/j.jenvman.2019.109895.

Chen, M., Ren, L., Qi, K., Li, Q., Lai, M., Li, Y., Li, X., Wang, Z., 2020. Enhanced removal of pharmaceuticals and personal care products from real municipal wastewater using an electrochemical membrane bioreactor. Bioresour. Technol. 311, 123579. https://doi.org/10.1016/j.biortech.2020.123579.

Comninellis, C., 1994. Electrocatalysis in the electrochemical conversion/combustion of organic pollutants for waste water treatment. Electrochim. Acta 39, 1857–1862. https://doi.org/10.1016/0013-4686(94)85175-1.

Costa, C.R., Montilla, F., Morallón, E., Olivi, P., 2009. Electrochemical oxidation of acid black 210 dye on the boron-doped diamond electrode in the presence of phosphate ions: effect of current density, pH, and chloride ions. Electrochim. Acta 54, 7048–7055. https://doi.org/10.1016/j.electacta.2009.07.027.

Cycoń, M., Markowicz, A., Borymski, S., Wójcik, M., Piotrowska-Seget, Z., 2013. Imidacloprid induces changes in the structure, genetic diversity and catabolic activity of soil microbial communities. J. Environ. Manag. 131, 55–65. https://doi.org/10.1016/j.jenvman.2013.09.041.

English, S.G., Sandoval-Herrera, N.I., Bishop, C.A., Cartwright, M., Maisonneuve, F., Elliott, J.E., Welch, K.C., 2021. Neonicotinoid pesticides exert metabolic effects on avian pollinators. Sci. Rep. 11, 1–11. https://doi.org/10.1038/s41598-021-82470-3.

European Comisssion, 2020. Neonicotinoids: current status of the neonicotinoids in the EU [WWW Document]. URL 3.16.21. https://ec.europa.eu/food/plant/pesticides/approval_active_substances/approval_renewal/neonicotinoids_en.

Feng, L., Oturan, N., van Hullebusch, E.D., Esposito, G., Oturan, M.A., 2014. Degradation of anti-inflammatory drug ketoprofen by electro-oxidation: comparison of electro-Fenton and anodic oxidation processes. Environ. Sci. Pollut. Res. 21, 8406–8416. https://doi.org/10.1007/s11356-014-2774-2.

Frontistis, Z., Antonopoulou, M., Yazirdagi, M., Kilinc, Z., Konstantinou, I., Katsaounis, A., Mantzavinos, D., 2017. Boron-doped diamond electro-oxidation of ethyl paraben: the effect of electrolyte on by-products distribution and mechanisms. J. Environ. Manag. 195, 148–156. https://doi.org/10.1016/j.jenvman.2016.06.044.

Ganiyu, S.O., Oturan, N., Raffy, S., Cretin, M., Esmilaire, R., van Hullebusch, E., Esposito, G., Oturan, M.A., 2016. Sub-stoichiometric titanium oxide (Ti_4O_7) as a suitable ceramic anode for electro-oxidation of organic pollutants: a case study of kinetics, mineralization and toxicity assessment of amoxicillin. Water Res. 106, 171–182. https://doi.org/10.1016/j.watres.2016.09.056.

García-espinoza, D., Mijaylova-nacheva, P., Avil, M., 2018. Electrochemical carbamazepine degradation : effect of the generated active chlorine , transformation pathways and toxicity. Chemosphere 192, 142–151. https://doi.org/10.1016/j.chemosphere.2017.10.147.

Humann-Guilleminot, S., Tassin de Montaigu, C., Sire, J., Grünig, S., Gning, O., Glauser, G., Vallat, A., Helfenstein, F., 2019. A sublethal dose of the neonicotinoid insecticide acetamiprid reduces sperm density in a songbird. Environ. Res. 177, 108589. https://doi.org/10.1016/j.envres.2019.108589.

Jardak, K., Dirany, A., Drogui, P., El Khakani, M.A., 2016. Electrochemical degradation of ethylene glycol in antifreeze liquids using boron doped diamond anode. Separ. Purif. Technol. 168, 215–222. https://doi.org/10.1016/j.seppur.2016.05.046.

Lakshmipathiraj, P., Bhaskar Raju, G., Sakai, Y., Takuma, Y., Yamasaki, A., Kato, S., Kojima, T., 2012. Studies on electrochemical detoxification of trichloroethene (TCE) on Ti/IrO_2-Ta_2O_5 electrode from aqueous solution. Chem. Eng. J. 198– 199, 211–218. https://doi.org/10.1016/j.cej.2012.05.092.

Lan, Y., Coetsier, C., Causserand, C., Groenen Serrano, K., 2017. On the role of salts for the treatment of wastewaters containing pharmaceuticals by electrochemical oxidation using a boron doped diamond anode. Electrochim. Acta 231, 309–318. https://doi.org/10.1016/j.electacta.2017.01.160.

Lopez-Antia, A., Ortiz-Santaliestra, M.E., Mougeot, F., Mateo, R., 2015. Imidacloprid-treated seed ingestion has lethal effect on adult partridges and reduces both breeding investment and offspring immunity. Environ. Res. 136, 97–107. https://doi.org/10.1016/j.envres.2014.10.023.

Louhichi, B., Ahmadi, M.F., Bensalah, N., Gadri, A., Rodrigo, M.A., 2008. Electrochemical degradation of an anionic surfactant on boron-doped diamond anodes. J. Hazard Mater. 158, 430–437. https://doi.org/10.1016/j.jhazmat.2008.01.093.

Montiel-León, J.M., Munoz, G., Vo Duy, S., Do, D.T., Vaudreuil, M.A., Goeury, K., Guillemette, F., Amyot, M., Sauvé, S., 2019. Widespread occurrence and spatial distribution of glyphosate, atrazine, and neonicotinoids pesticides in the St. Lawrence and tributary rivers. Environ. Pollut. 250, 29–39. https://doi.org/10.1016/j.envpol.2019.03.125.

Nájera-Aguilar, H.A., Gutiérrez-Hernández, R.F., De Los Santos, R.G., García-Lara, C., Méndez-Novelo, R., Rojas-Valencia, M.N., 2016. Degradation of gestodene (GES)-17A-ethinylestradiol (EE2) mixture by electrochemical oxidation. J. Water Health 14, 980–988. https://doi.org/10.2166/wh.2016.104.

Nidheesh, P.V., Gandhimathi, R., 2012. Trends in electro-Fenton process for water and wastewater treatment: an overview. Desalination 299, 1–15. https://doi.org/10.1016/j.desal.2012.05.011.

Ouarda, Y., Bouchard, F., Azaïs, A., Vaudreuil, M.A., Drogui, P., Dayal Tyagi, R., Sauvé, S., Buelna, G., Dubé, R., 2019. Electrochemical treatment of real hospital wastewaters and monitoring of pharmaceutical residues by using surrogate models. J. Environ. Chem. Eng. 7, 103332. https://doi.org/10.1016/j.jece.2019.103332.

Panizza, M., Cerisola, G., 2005. Application of diamond electrodes to electrochemical processes. Electrochim. Acta 51, 191–199. https://doi.org/10.1016/j.electacta.2005.04.023.

Pueyo, N., Ormad, M.P., Miguel, N., Kokkinos, P., Ioannidi, A., Mantzavinos, D., Frontistis, Z., 2020. Electrochemical oxidation of butyl paraben on boron doped diamond in environmental matrices and comparison with sulfate radical-AOP. J. Environ. Manag. 269, 110783. https://doi.org/10.1016/j.jenvman.2020.110783.

Rajasekhar, B., Venkateshwaran, U., Durairaj, N., Divyapriya, G., Nambi, I.M., Joseph, A., 2020. Comprehensive treatment of urban wastewaters using electrochemical advanced oxidation process. J. Environ. Manag. 266, 110469. https://doi.org/10.1016/j.jenvman.2020.110469.

Samet, Y., Agengui, L., Abdelhédi, R., 2010. Electrochemical degradation of chlorpyrifos pesticide in aqueous solutions by anodic oxidation at boron-doped diamond electrodes. Chem. Eng. J. 161, 167–172. https://doi.org/10.1016/j.cej.2010.04.060.

Simon-Delso, N., Amaral-Rogers, V., Belzunces, L.P., Bonmatin, J.M., Chagnon, M., Downs, C., Furlan, L., Gibbons, D.W., Giorio, C., Girolami, V., Goulson, D., Kreutzweiser, D.P., Krupke, C.H., Liess, M., Long, E., McField, M., Mineau, P., Mitchell, E.A.D., Morrissey, C.A., Noome, D.A., Pisa, L., Settele, J., Stark, J.D., Tapparo, A., Van Dyck, H., Van Praagh, J., Van der Sluijs, J.P., Whitehorn, P.R., Wiemers, M., 2015. Systemic insecticides (neonicotinoids and fipronil): trends, uses, mode of action and metabolites. Environ. Sci. Pollut. Res. 22, 5–34. https://doi.org/10.1007/s11356-014-3470-y.

Sirés, I., Brillas, E., Oturan, M.A., Rodrigo, M.A., Panizza, M., 2014. Electrochemical advanced oxidation processes: today and tomorrow. A review. Environ. Sci. Pollut. Res. 21, 8336–8367. https://doi.org/10.1007/s11356-014-2783-1.

Sjerps, R.M.A., Kooij, P.J.F., van Loon, A., Van Wezel, A.P., 2019. Occurrence of pesticides in Dutch drinking water sources. Chemosphere 235, 510–518. https://doi.org/10.1016/j.chemosphere.2019.06.207.

Tang, Y., He, D., Guo, Y., Qu, W., Shang, J., Zhou, L., Pan, R., Dong, W., 2020. Electrochemical oxidative degradation of X-6G dye by boron-doped diamond anodes: effect of operating parameters. Chemosphere 258, 127368. https://doi.org/10.1016/j.chemosphere.2020.127368.

Tasman, K., Hidalgo, S., Zhu, B., Rands, S.A., Hodge, J.J.L., 2021. Neonicotinoids disrupt memory, circadian behaviour and sleep. Sci. Rep. 11, 1–13. https://doi.org/10.1038/s41598-021-81548-2.

Turan, A., Keyikoglu, R., Kobya, M., Khataee, A., 2020. Degradation of thiocyanate by electrochemical oxidation process in coke oven wastewater: role of operative parameters and mechanistic study. Chemosphere 255. https://doi.org/10.1016/j.chemosphere.2020.127014.

Yin, K., Deng, Y., Liu, C., He, Q., Wei, Y., Chen, S., Liu, T., Luo, S., 2018. Kinetics, pathways and toxicity evaluation of neonicotinoid insecticides degradation via UV/chlorine process. Chem. Eng. J. 346, 298–306. https://doi.org/10.1016/j.cej.2018.03.168.

Zazou, H., Oturan, N., Zhang, H., Hamdani, M., Oturan, M.A., 2017. Comparative study of electrochemical oxidation of herbicide 2,4,5-T: kinetics, parametric optimization and mineralization pathway. Sustain. Environ. Res. 27, 15–23. https://doi.org/10.1016/j.serj.2016.11.008.

Zhang, T., Song, S., Bai, X., He, Y., Zhang, B., Gui, M., Kannan, K., Lu, S., Huang, Y., Sun, H., 2019. A nationwide survey of urinary concentrations of neonicotinoid insecticides in China. Environ. Int. 132, 105114. https://doi.org/10.1016/j.envint.2019.105114.